

Random Numerical Methods for Free Boundary Models in Population Dynamics

V. Egorova^{‡,1} M.-C. Casabán^b R. Company^b and L. Jódar^b

(‡) Depto. de Matemática Aplicada y Ciencias de la Computación, Universidad de Cantabria
Avda. de los Castros, s/n, Santander, Spain

(b) I.U. de Matemática Multidisciplinar, Universitat Politècnica de València
Camí de Vera s/n, València, Spain.

1 Introduction

In this study, we introduce random numerical methods for a stochastic extension of the free boundary diffusive logistic model with radial symmetry as proposed in [1, 2]. In these models, certain parameters, such as the growth rate or diffusion coefficient are assumed random due to the inherent variability in natural phenomena. Hence, the system's behaviour influenced by this randomness, results in solutions that themselves are stochastic processes (s.p.'s). The position of the free boundary is determined by the interplay among population growth, diffusion characteristics, and randomly varying environmental parameters. Consequently, the free boundary becomes a s.p., adding an additional layer of complexity to the models. In our approach, we adopt a stochastic methodology based on mean square (m.s.) calculus, where uncertainty is well-defined.

The random population density of a spreading species, denoted as $u(\omega) = u(r, t; \omega)$, and the random moving boundary, $H(t; \omega)$, are both stochastic processes defined in a complete probability space $(\Omega, \mathcal{F}, \mathbb{P})$. Following prior research on random moving boundary phase-change problems [3], we limit the uncertainty to p -degrees of randomness, where p represents the dependence on a finite number of random variables (r.v.'s) [4, p.37].

Inspired in the seminal radially symmetry deterministic model [1], this paper is focused on the following random free boundary diffusive logistic model of Stefan type in the m.s. sense:

$$u_t(\omega) = D(\omega) \left(u_{rr}(\omega) + \frac{1}{r} u_r(\omega) \right) + u(\omega) (\alpha(r) - \beta(r) u(\omega)), \quad t > 0, 0 < r < H(t; \omega), \omega \in \Omega, \quad (1)$$

$$H'(t; \omega) = -\eta(\omega) u_r(H(t; \omega), t; \omega), \quad t > 0, \omega \in \Omega, \quad (2)$$

subject to the initial and boundary conditions

$$H(0; \omega) = H_0, \quad u(r, 0; \omega) = u_0(r), \quad 0 \leq r \leq H_0, \quad (3)$$

$$u_r(0, t; \omega) = 0, \quad u(H(t; \omega), t; \omega) = 0, \quad t > 0. \quad (4)$$

The positive random variable (r.v.) $D(\omega) > 0$ in the random partial differential equation (RPDE) (1) denotes the diffusion rate and it is bounded such that

$$0 < d_1 \leq D(\omega) \leq d_2, \quad \text{for every } \omega \in \Omega. \quad (5)$$

¹vera.egorova@unican.es

The r.v. $\eta(\omega)$, in the Stefan condition (2), denotes a positive r.v. meaning the proportionality between the random moving boundary speed, $H'(t; \omega)$, and the random population gradient at the front. It is assumed there exists a bound η_0 such that

$$0 < \eta_0 \leq \eta(\omega), \text{ for every } \omega \in \Omega. \quad (6)$$

The function $\alpha(r)$ is the intrinsic growth rate and $\alpha(r)/\beta(r)$ is the habitat carrying capacity of the species. Both, $\alpha(r)$ and $\beta(r)$ are bounded continuous real functions satisfying

$$\exists \kappa_1, \kappa_2 > 0 : \quad \kappa_1 \leq \alpha(r), \beta(r) \leq \kappa_2, \quad \forall r \in [0, \infty). \quad (7)$$

Moreover, initial population density function $u_0(r)$ satisfies

$$u_0 \in C^2([0, H_0]), \quad u_0'(0) = u_0(H_0) = 0, \quad u_0(r) > 0, \quad \forall r \in [0, H_0]. \quad (8)$$

H_0 is the radius value for the circular region where the initial population is confined.

The aim of this paper is to construct stable numerical finite difference schemes (RFDS's) for the random diffusive logistic model (1)–(8) preserving the qualitative characteristics of its solution. Specifically, we focus on the study and the comparison of two random numerical methods: the random Front-Fixing (FF) method and the random Front-Tracking (FT) method.

Iterative methods like finite difference schemes face challenges in random scenarios due to storage complexities from symbolic computations of stochastic processes [5]. To address this, we combine sample mean square methodology with the Monte Carlo method for efficient computation of statistical moments [6]. To speed up the computational process, which becomes particularly crucial when dealing with large-scale Monte Carlo simulations, we have employed a parallel computing environment.

2 Random Numerical Methods

2.1 A random FF method

In this section we present a random FF method based on Landau-type transformation together with the construction of a random explicit finite difference scheme (RFDS) for solve numerically the radial symmetric diffusive logistic model (1)–(8). Let us use the change of variables,

$$z = \frac{r}{H(t; \omega)}, \quad v(z, t; \omega) = u(r, t; \omega). \quad (9)$$

Note that the new spatial variable z is a fixed proportion $0 \leq z \leq 1$ for each $r \in [0, H(t; \omega)]$ at fixed time $t > 0$. From this point of view, the original spatial variable $r = zH(t; \omega)$ depends on every event $\omega \in \Omega$ and it becomes a r.v. for every fixed t . Moreover, deterministic parameters $\alpha(r)$ and $\beta(r)$ become random ones as well: $\alpha(r) = \alpha(zH(t; \omega)) = a(z, t; \omega)$, $\beta(r) = \beta(zH(t; \omega)) = b(z, t; \omega)$, with the same constraint $0 < \kappa_1 \leq a(z, t; \omega)$, $b(z, t; \omega) \leq \kappa_2$, $t > 0$, $0 \leq z \leq 1$, $\omega \in \Omega$.

By denoting $G(t; \omega) = H^2(t; \omega)$ and substituting (9) into the problem (1)–(4), one gets for $t > 0$, $0 < z < 1$, $\omega \in \Omega$,

$$G(t; \omega) v_t = D(\omega) v_{zz} + \left(\frac{D(\omega)}{z} + \frac{z}{2} G'(t; \omega) \right) v_z + G(t; \omega) [a(z, t; \omega) - b(z, t; \omega) v] v, \quad (10)$$

$$G'(t; \omega) = -2\eta(\omega) v_z(1, t; \omega), \quad t > 0, \omega \in \Omega, \quad (11)$$

subject to the initial and boundary conditions

$$G(0) = H_0^2, \quad v(z, 0) = u_0(zH_0^2), \quad v_z(0, t; \omega) = 0, \quad v(1, t; \omega) = 0, \quad t > 0, \quad 0 \leq z \leq 1, \quad \omega \in \Omega. \quad (12)$$

Note that s.p.'s v^2 , v_z , v_t , v_{zz} , $G(t; \omega)$ and $G'(t; \omega)$ lie in $L_4(\Omega)$ in order to legitimised the m.s. operational calculus developed in (10)–(11).

Construction of RFDS-FF

We consider the transformed problem (10)–(12). Let us define a uniform grid $z_j = jh$, $h = 1/M$, $t^n = nk$, $k = T/N$, where N and M are two given positive integer numbers and T is a fixed time horizon. We denote by $v_j^n(\omega) \approx v(z_j, t^n; \omega)$ the numerical approximation of the solution s.p. $v(z, t; \omega)$, $\omega \in \Omega$, in a mesh point (z_j, t^n) . In addition we introduce the following notation

$$g^n(\omega) \approx G(t^n; \omega), \quad a_j^n(\omega) = a(z_j, t^n; \omega), \quad b_j^n(\omega) = b(z_j, t^n; \omega).$$

By using a forward first-order approximation for the m.s. time derivatives and a centred second-order approximations for the m.s. spatial derivatives, one gets the following RFDS-FF for the problem (10)–(12):

$$v_j^{n+1}(\omega) = A_j^n(\omega) v_{j-1}^n(\omega) + B_j^n(\omega) v_j^n(\omega) + C_j^n(\omega) v_{j+1}^n(\omega), \quad 1 \leq j \leq M-1, \quad 0 \leq n \leq N-1, \quad \omega \in \Omega, \quad (13)$$

where

$$\left. \begin{aligned} A_j^n(\omega) &= \frac{D(\omega)k}{h^2 g^n(\omega)} - \frac{D(\omega)k}{2h g^n(\omega) z_j} - \frac{z_j}{4h} \left(\frac{g^{n+1}(\omega)}{g^n(\omega)} - 1 \right) \\ B_j^n(\omega) &= 1 + k \left(a_j^n(\omega) - b_j^n(\omega) v_j^n(\omega) - \frac{2D(\omega)k}{h^2 g^n(\omega)} \right) \\ C_j^n(\omega) &= \frac{D(\omega)k}{h^2 g^n(\omega)} + \frac{D(\omega)k}{2h g^n(\omega) z_j} + \frac{z_j}{4h} \left(\frac{g^{n+1}(\omega)}{g^n(\omega)} - 1 \right) \end{aligned} \right\} \quad 0 \leq n \leq N-1, \quad \omega \in \Omega; \quad (14)$$

$$\frac{g^{n+1}(\omega) - g^n(\omega)}{k} = -\frac{\eta(\omega)}{h} (3v_M^n(\omega) - 4v_{M-1}^n(\omega) + v_{M-2}^n(\omega)), \quad 0 \leq n \leq N-1. \quad (15)$$

Boundary conditions (12) are discretized as

$$v_z(0, t^n; \omega) \approx \frac{-3v_0^n(\omega) + 4v_1^n(\omega) - v_2^n(\omega)}{2h} = 0, \quad v_M^n(\omega) = 0, \quad 0 \leq n \leq N. \quad (16)$$

Once numerical solution for the transformed RPDE (10)–(12) is computed, the numerical solution of the original random Stefan problem (1)–(8) at $t = T$ is found by the inverse transformation: $r_j \approx z_j H(T; \omega)$, $u(r_j, T; \omega) \approx v_j^N(\omega)$.

Qualitative properties of the numerical solutions s.p.'s

Now we present qualitative properties of the RFDS-FF (13)–(16), such as conditional stability, positivity and monotonicity of the random numerical s.p.'s. For the sake of clarity in the presentation, we recall some definitions [3].

Definition 1 *The numerical solution s.p. $\{v_j^n(\omega)\}$, $\omega \in \Omega$, of a random RFDS is said to be non-increasing monotone in the spatial index $j = 0, \dots, M-1$, if $v_j^n(\omega_\ell) \geq v_{j+1}^n(\omega_\ell)$, for $0 \leq j \leq M-1$, $0 \leq n \leq N$, $\forall \omega_\ell \in \Omega$.*

Definition 2 *The numerical free boundary s.p. $\{g^n(\omega)\}$, $\omega \in \Omega$ of a random RFDS is said to be strictly increasing, if $g^n(\omega_\ell) < g^{n+1}(\omega_\ell)$, $0 \leq n \leq N-1$, $\forall \omega_\ell \in \Omega$.*

Definition 3 *A random numerical scheme is said to be $\|\cdot\|_p$ -stable in the fixed station sense in $[0, 1] \times [0, T]$, if for every partition with $k = T/N$ and $h = 1/M$, it is fulfilled that*

$$\|v_j^n(\omega_\ell)\|_p \leq C, \quad 0 \leq j \leq M, \quad 0 \leq n \leq N, \quad \forall \omega_\ell \in \Omega, \quad (17)$$

where the constant C is independent of the step-sizes h and k the time level n .

In [7], the free boundary diffusive logistic model was studied in the deterministic scenario proposing the Front-Fixing method combined with a finite difference scheme. Numerical analysis developed provides qualitative properties of the numerical solution summarized in Theorems 2-6 of [7]. In the present random scenario, we apply those theorems taking into account that $D(\omega) > 0$ is a bounded r.v. verifying condition $D(\omega) < d_2$ for every $\omega \in \Omega$, as given in (5). Then the following result is established.

Theorem 1 *With the previous notation for small enough spatial step-size h , the random numerical solution $\{v_j^n(\omega)\}$, $\omega \in \Omega$, is positive $0 \leq j \leq M$, $0 \leq n \leq N$; non-increasing monotone in the spatial index j . Moreover, the random free-boundary s.p. $\{g^n(\omega)\}$, $\omega \in \Omega$, is strictly increasing. Finally, $\{v_j^n(\omega)\}$ is $\|\cdot\|_p$ -stable in the fixed station sense if $k < Qh^2$, $Q = \min_{1 \leq i \leq 3} Q_i$, where*

$$Q_1 = \frac{H_0^2}{2d_2 + h^2 \alpha_1 H_0^2 \left(\frac{\alpha_2 \beta_2}{\alpha_1 \beta_1} - 1 \right)}; \quad Q_2 = \frac{H_0^2}{2d_2 + h^2 \beta_2 H_0^2 (2M_0 - C_m)}; \quad Q_3 = \frac{4H_0^2}{9d_2 + 8h^2 \beta_2 H_0^2 P_0};$$

$$C_0 = \sup_{r \in \mathbb{R}^+} \left\{ \frac{\alpha(r)}{\beta(r)} \right\}, \quad C_m = \inf_{r \in \mathbb{R}^+} \left\{ \frac{\alpha(r)}{\beta(r)} \right\}, \quad M_0 = \max_{0 \leq r \leq H_0} \{u_0(r)\}, \quad P_0 = \max \{M_0, C_0\},$$

and $\alpha_i, \beta_i, i = 1, 2$, verify

$$0 < \kappa_1 \leq \alpha_1 \leq \alpha(r) \leq \alpha_2 \leq \kappa_2, \quad 0 < \kappa_1 \leq \beta_1 \leq \beta(r) \leq \beta_2 \leq \kappa_2, \quad \forall r \in [0, \infty). \quad (18)$$

2.2 A random FT method

In this section we propose a random FT method for the RPDE (1)–(8), employing the fixed grid approach, where the space-time domain is subdivided into a finite number of uniformly distributed nodes and the position of the boundary does not necessarily coincide with the mesh points. We consider the numerical domain $[0, L] \times [0, T]$, with the grid points $r_j = jh$, $t^n = nk$, where h and k are the space and time increments, respectively. The step sizes (h, k) are fixed and it appears a fractional distance between the last interior mesh point and the localization of the moving boundary. The numerical approximation of the solution s.p. $u(r_j, t^n; \omega)$ is denoted by $u_j^n(\omega)$ and the approximation of the moving front s.p. $H(t^n; \omega)$ is denoted by $H^n(\omega)$. Let us denote $i^n(\omega)$ the spatial index of the last interior point of the non-zero population region, that is, $r_{i^n(\omega)} < H^n(\omega) \leq r_{i^n(\omega)+1}$, $\omega \in \Omega$.

Then, for any realization $\omega \in \Omega$, there exists a distance parameter in each time level n namely $p^n(\omega)$, such that

$$H^n(\omega) = (i^n(\omega) + p^n(\omega))h, \quad 0 < p^n(\omega) \leq 1, \quad 0 \leq n \leq N. \quad (19)$$

From (3) one gets $H^0(\omega) = H_0$ and for initialization we take $p^0(\omega) = p^0 = 1$, $i^0(\omega) = i^0 = M - 1$ and $H^0(\omega) = H_0 = (i^0 + 1)h = Mh$, for all realizations $\omega \in \Omega$.

In order to approximate the m.s. spatial partial derivatives of the RPDE (1) at the last interior point $r_{i^n(\omega)} = i^n(\omega)h$, a Lagrange interpolation passing through the points $r_{i^n(\omega)-1}$, $r_{i^n(\omega)}$ and $H^n(\omega)$ is used, see [8, Pages 164-165], obtaining the approximations

$$\frac{\partial^2 u}{\partial r^2}(r_{i^n(\omega)}, t^n; \omega) \approx \frac{2}{h^2} \left(\frac{1}{p^n(\omega) + 1} u_{i^n(\omega)-1}^n(\omega) - \frac{1}{p^n(\omega)} u_{i^n(\omega)}^n(\omega) \right), \quad (20)$$

$$\frac{\partial u}{\partial r}(r_{i^n(\omega)}, t^n; \omega) \approx \frac{1}{h} \left(-\frac{p^n(\omega)}{1 + p^n(\omega)} u_{i^n(\omega)-1}^n(\omega) - \frac{1 - p^n(\omega)}{p^n(\omega)} u_{i^n(\omega)}^n(\omega) \right), \quad (21)$$

In the boundary $H^n(\omega)$, see (19), the same three point Lagrange interpolation formulae provides the following m.s. approximation for the first spatial m.s. derivative at the moving front involved in Stefan condition (2)

$$\frac{\partial u}{\partial r}(H^n(\omega), t^n; \omega) \approx \frac{1}{h} \left(\frac{p^n(\omega)}{p^n(\omega) + 1} u_{i^n(\omega)-1}^n(\omega) - \frac{p^n(\omega) + 1}{p^n(\omega)} u_{i^n(\omega)}^n(\omega) \right). \quad (22)$$

The forward approximation of the time m.s. derivative in (2)

$$\frac{d}{dt}(H(t^n; \omega)) \approx \frac{H^{n+1}(\omega) - H^n(\omega)}{k} = \frac{(\Delta^n(\omega) - p^n(\omega)) h}{k} \quad (23)$$

where $\Delta^n(\omega) h$ denotes the distance between the last interior point in the time level n and the localization of the moving front in time level $n + 1$, that is

$$\Delta^n(\omega) h = H^{n+1}(\omega) - i^n(\omega) h. \quad (24)$$

From the approximations above the discretization of the RPDE (1) takes the following form:

- For $1 \leq j \leq i^n(\omega) - 1$:

$$u_j^{n+1}(\omega) = \tilde{A}_j^n(\omega) u_{j-1}^n(\omega) + \tilde{B}_j^n(\omega) u_j^n(\omega) + \tilde{C}_j^n(\omega) u_{j+1}^n(\omega), \quad (25)$$

where

$$\left. \begin{aligned} \tilde{A}_j^n(\omega) &= \frac{k D(\omega)}{h^2} \left(1 - \frac{1}{2j}\right) > 0, & \tilde{C}_j^n(\omega) &= \frac{k D(\omega)}{h^2} \left(1 + \frac{1}{2j}\right) > 0, \\ \tilde{B}_j^n(\omega) &= 1 + k \left[-\frac{2D(\omega)}{h^2} + \alpha_j - \beta_j u_j^n(\omega)\right], & \text{with } \alpha_j &= \alpha(r_j), \beta_j = \beta(r_j). \end{aligned} \right\} \quad (26)$$

- For the last interior point $r_{i^n(\omega)} = i^n(\omega) h$, we use the approximations (20) and (21) obtaining

$$\begin{aligned} u_{i^n(\omega)}^{n+1}(\omega) &= u_{i^n(\omega)}^n(\omega) + k \frac{D(\omega)}{h^2} \left[\frac{u_{i^n(\omega)-1}^n(\omega)}{p^n(\omega) + 1} \left(2 - \frac{p^n(\omega)}{i^n(\omega)}\right) - \frac{u_{i^n(\omega)}^n(\omega)}{p^n(\omega)} \left(2 + \frac{1 - p^n(\omega)}{i^n(\omega)}\right) \right] \\ &\quad + k u_{i^n(\omega)}^n(\omega) \left(\alpha_{i^n(\omega)} - \beta_{i^n(\omega)} u_{i^n(\omega)}^n(\omega)\right). \end{aligned} \quad (27)$$

- For $j = 0$: $u_0^{n+1}(\omega) = \frac{4 u_1^{n+1}(\omega) - u_2^{n+1}(\omega)}{3}$
- For the advance of the front, given by the Stefan condition (2), from the approximations (23)–(24) it results that

$$\Delta^n(\omega) = p^n(\omega) + \frac{k \eta(\omega)}{h^2} \left(\frac{p^n(\omega) + 1}{p^n(\omega)} u_{i^n(\omega)}^n(\omega) - \frac{p^n(\omega)}{p^n(\omega) + 1} u_{i^n(\omega)-1}^n(\omega) \right). \quad (28)$$

Then the moving front at time level $n + 1$ is given by

$$H^{n+1}(\omega) = (i^n(\omega) + \Delta^n(\omega)) h. \quad (29)$$

Stability condition for the RFDS-FT (25)–(29) has been found in order to guarantee the m.s. stability of the pairwise solution s.p.'s $\{u_j^n(\omega), H(t^n; \omega)\}$:

$$k \leq \min \left\{ \frac{h}{\eta_0 |u_0'(H_0)|}, \frac{h^2}{2d_2 + |\alpha_1 - \beta_2 P_0| h^2}, \frac{\epsilon h^2 i^0}{d_2 (2i^0 + 1 - \epsilon)} \right\}, \quad (30)$$

where d_2 is defined in (5), η_0 is given by (6), α_1 and β_2 are defined in (18), and P_0 is defined in Theorem 1.

3 Numerical Results

In this section, we compare the numerical results from RFDS-FF and RFDS-FT methods. We chose $\alpha = \beta = 1$, $H_0 = 3$, $D(\omega) \sim \mathcal{N}_{[0.8, 1.2]}(1, 0.1)$ and $\eta(\omega) \sim \mathcal{B}e_{[1.6, 2.4]}(2, 4)$. Note that we have chosen truncated distributions for the s.v.'s $D(\omega)$ and $\eta(\omega)$ because of the boundedness conditions (5) and (6). The initial population distribution is given by $u_0(r) = \cos\left(\frac{\pi r}{6}\right)$.

Taking $M = 50$ spatial points, resulting in $h_{FF} = \frac{1}{M} = \frac{1}{50}$ and $h_{FT} = \frac{H_0}{M} = \frac{3}{50}$, respectively, we consider the following time step-size $k = 7.0e - 04$ to ensure satisfaction of the hypothesis of Theorem 1 and condition (30) simultaneously, which means the stability of the solutions s.p. generated for both methods.

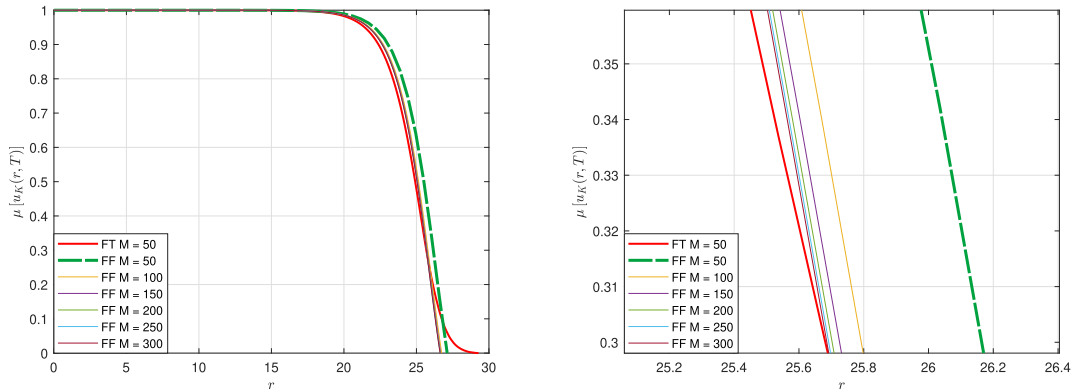


Figure 1: Mean of the numerical solution s.p. for the problem (1)–(8) at $T = 50$, comparing the FF method with different numbers of grid points M , and the FT method using $M = 50$ grid points. The plot on the right shows a zoomed-in view.

Figure 1 displays the mean of the numerical solution for problem (1)–(8). It compares the RFDS-FF method with various numbers of grid points M , against the RFDS-FT method that uses $M = 50$ grid points. Up to the inflection point, represented by the average of the free boundary as calculated by the FT method, the results exhibit convergence patterns. For short time intervals, both methods give similar results.

In the study of errors of the free random boundary, $H(t; \omega)$, we use the following absolute deviations

$$\begin{aligned} \text{AbsDev}(\mu[H_K^{FF}, H_K^{FT}]) &= |\mu[H^{FF}(t; \omega_K)] - \mu[H^{FT}(t; \omega_K)]|, \quad 0 \leq t \leq T, \quad K \text{ fixed}, \\ \text{AbsDev}(\sigma[H_K^{FF}, H_K^{FT}]) &= |\sigma[H^{FF}(t; \omega_K)] - \sigma[H^{FT}(t; \omega_K)]|, \quad 0 \leq t \leq T, \quad K \text{ fixed}. \end{aligned} \quad (31)$$

Figure 2 shows that the approximations of both statistical moments of the free boundary the mean, $\mu[H(t; \omega_K)]$, and the standard deviation $\sigma[H(t; \omega_K)]$ computed by means of the random FF and FT methods are close independently of the number of Monte Carlo simulations K . Note that in these figures we illustrate the full evolution of the absolute deviations of the statistical moments of the free boundary up to the times $T = 1$ and $T = 10$, respectively.

The statistical spread of the numerical solution s.p. is sensitive to the changes of the standard deviation of the involved r.v.'s data in the model, i.e. the random parameters $D(\omega)$ and $\eta(\omega)$. Taking $M = 50$, $K = 100$, and $T = 10$ and the distribution $\mathcal{N}_{[0.8, 1.2]}(1, 0.1)$ for $D(\omega)$, Figure 3(left) shows the standard deviation of the numerical solution s.p. for different pairs of the parameters

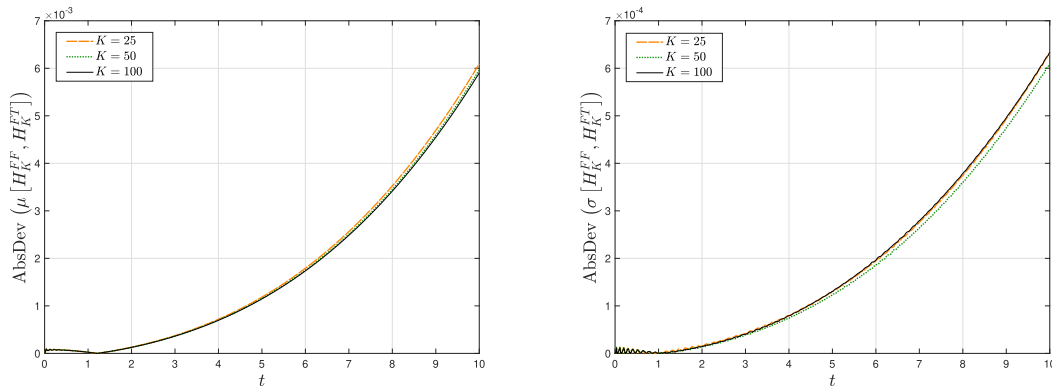


Figure 2: Absolute deviations of the mean (left) and the standard deviation (right) of the random free boundary $H(T; \omega_K)$ computed between RFDS-FF and RFDS-FT methods up to time $T = 10$ by (31) when the sample K realizations varies.

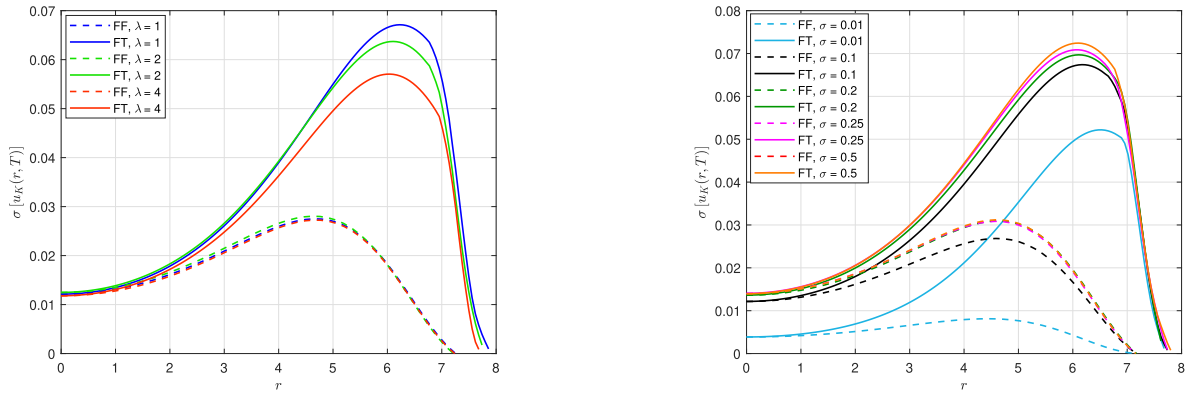


Figure 3: Standard deviation of numerical solution s.p. computed by the FF (solid lines) and FT (dashed lines) methods for $T = 10$. Left plot: over different $\lambda = 1, 2, 4$ in $\mathcal{B}_{[1.6, 2.4]}(2\lambda, 4\lambda)$. Right plot: over different $\sigma = 0.01, \dots, 0.5$ in $\mathcal{N}_{[0.8, 1.2]}(1, \sigma)$.

of the shifted-beta distribution. In an analogous way, fixing the distribution $\mathcal{B}_{[1.6, 2.4]}(2, 4)$ for $\eta(\omega)$, the the standard deviation of the numerical solution s.p. for various values of the parameter σ in the truncated normal distribution $\mathcal{N}_{[0.8, 1.2]}(1, \sigma)$ is shown in Figure 3 (right). A consistent behavioural pattern is observed across all cases. As we get closer to the free boundary, the standard deviation also moves towards zero, as for all realizations the population density becomes zero when the spatial variable reaches the moving front.

4 Conclusions

This paper introduces a random free boundary diffusive logistic model with radial symmetry, considering parameters with finite randomness and a random unknown function for the propagation front. Two random approaches, the front-fixing (FF) and front-tracking (FT) methods, are utilized to handle the free boundary. Numerical solutions employ explicit RFDS, with stability and positivity conditions established for both methods.

RFDS in the mean square sense poses storage issues due to computing expectation and variance iteratively. To address this, the Monte Carlo technique is employed for computing statistical moments of the solution and stochastic moving boundary.

The study compares the proposed methods, identifying advantages, drawbacks, and applicability areas. The RFDS-FF method requires a fixed number of grid points for all time iterations and sample realizations, while the RFDS-FT method adapts grid points dynamically. Despite being more efficient in time and memory usage, the RFDS-FF method may sacrifice accuracy due to fixed boundary inverse transformation, mitigated by using more grid points. In contrast, the RFDS-FT method maintains consistent step-size, eliminating this drawback.

In conclusion, the choice between RFDS-FF and RFDS-FT methods depends on the specific problem. The RFDS-FF method suits smaller time simulations requiring fast and accurate results, while the RFDS-FT method is preferable for longer time horizons. By understanding the strengths and limitations, researchers can select the most suitable approach for their application.

Acknowledgments

This work has been partially supported by the Spanish Ministry of Economy and Competitiveness MINECO through the project PID2019-107685RB-I00 and by the Spanish State Research Agency (AEI) through the project PDC2022-133115-I00.

References

- [1] Y. Du, Z. Guo, Spreading-vanishing dichotomy in a diffusive logistic model with a free boundary, II, *Journal of Differential Equations* 250 (2011) 4336–4366. doi:10.1016/j.jde.2011.02.011.
- [2] S. Liu, Y. Du, X. Liu, Numerical studies of a class of reaction-diffusion equations with Stefan conditions, *International Journal of Computer Mathematics* 97 (5) (2020) 959–979. doi:10.1080/00207160.2019.1599868.
- [3] M. C. Casabán, R. Company, L. Jódar, Numerical difference solution of moving boundary random Stefan problems, *Mathematics and Computers in Simulations* 205 (2023) 878–901. doi:10.1016/j.matcom2022.10.026.
- [4] T. Soong, *Random Differential Equations in Science and Engineering*, Academic Press: New-York, USA, 1973.
- [5] M. C. Casabán, R. Company, L. Jódar, Reliable efficient difference methods for random heterogeneous diffusion reaction models with a finite degree of randomness, *Mathematics* 206 (2021) 351–366. doi:10.3390/math9030206.
- [6] D. P. Kroese, T. Taimre, Z. I. Botev, *Handbook of Monte Carlo Methods*, John Wiley et Sons Ltd., 2011.
- [7] M. C. Casabán, R. Company, V. N. Egorova, L. Jódar, Qualitative numerical analysis of a free-boundary diffusive logistic model, *Mathematics* 11 (2023). doi:10.3390/math11061296.
- [8] J. Crank, *Free and Moving Boundary problems*, Oxford University Press, 1984.